Machine-vision-based electrode wear analysis for closed-loop wire EDM process control

Abhilash P. M.*, D. Chakradhar

Department of Mechanical Engineering, Indian Institute of Technology Palakkad, Kerala, India, 678557

*Corresponding author: abhilashpm184@gmail.com, ORCID ID: 0000-0001-5655-6196

Abstract: The purpose of this study was to develop a closed-loop machine vision system for wire electrical discharge machining (EDM) process control. Excessive wire wear leading to wire breakage is the primary cause of wire EDM process failures. Such process interruptions are undesirable because they affect cost efficiency, surface quality, and process sustainability. The developed system monitors wire wear using an image-processing algorithm and suggests parametric changes according to the severity of the wire wear. Microscopic images of the wire electrode coming out from the machining zone are fed to the system as raw images. In the proposed method, the images are pre-processed and enhanced to obtain a binary image that is used to compute the wire wear ratio. The input parameters that are adjusted to recover from the unstable conditions that cause excessive wire wear are pulse off time, servo voltage, and wire feed rate. The algorithm successfully predicted wire breakage events. In addition, the alternative parametric settings proposed by the control algorithm were successful in reducing the wire wear to safe limits, thereby preventing wire breakage interruptions.

Keywords: Wire electrical discharge machining; machine vision; image processing; wire wear; wire electrode; wire breakage; Inconel 718; process control

1. Introduction

Wire electrical discharge machining (WEDM) is a nontraditional machining technique that uses controlled and repeated spark erosion for material removal. The material removal is noncontact in nature; thus, even the hardest materials can be machined with negligible mechanical residual stresses and cutting forces. Even though the process has many advantages compared with conventional processes, process interruptions and failures associated with the process have been reported extensively [1, 2]. Many researchers have attempted to optimize the process parameters to maximize process performance [3–6]. However, the process characteristics are material dependent, and it is difficult to optimize the process overall. In addition, the stochastic nature of the process and complex interactions make the process

challenging to control [7]. One common cause of process interruption is wire breakage. Wire breakages cause excessive energy consumption, waste material, and reduce process performance [8]. They are also associated with machined surface damage, geometric inaccuracy, and subsequent part rejection [9]. Predictive models capable of early detection of process instability leading to wire breakage are relevant in this regard. Timely regulation of spark gap conditions can restore process stability by avoiding debris accumulation and subsequent short-circuit discharges [10]. Although several attempts have been made to develop process control systems, such failures have not been eradicated completely. In this regard, an image-processing-based wire wear detection and process control methodology was developed in this study.

2. Literature Review

Many process-monitoring techniques have been developed in the past to predict and control wire breakages. Kwon and Yang [11] developed a model to predict process stability based on the instantaneous energy of the discharge pulse. The model aims to prevent wire breakages and enhance transient stability by real-time monitoring of current and voltage pulses. A few researchers have attempted fuzzy-logic-based WEDM control strategies [12–14]. A fuzzy-logic-based hybrid offline–online process-monitoring method was proposed by Bufardi et al. [15]. The model predicts surface damage and takes automatic preventive measures by adjusting the pulse off time. However, fuzzy-logic models are rule-based and cannot be tuned based on training data, which may limit the accuracy of the model. Caggiano et al. [16] emphasized the importance of considering a number of features by sensor fusion to understand and predict defects completely. They developed strategies to extract and evaluate 10 different parameters based on the features extracted from voltage and current signals. However, computing these features in real time can be computationally challenging and expensive. Cabenes et al. [17] developed a control strategy to alert users based on the severity of the machining instability to forecast wire breakages. The proposed method is capable of early detection of wire breakages based on spark energy, ignition delay, and discharge current amplitude. The system can alert users, but it does not include a control strategy to improve the stability situation. Klocke et al. [18] developed a process-monitoring method to control the surface finish of WEDM-processed Inconel 718. The threshold values of the mean gap voltage were found experimentally to maintain a certain level of surface finish. Then, the mean gap voltage of the spark gap was monitored in real time, and surface defects were observed whenever the set thresholds were breached.

Many researchers have used image-processing techniques to identify and quantify surface features during manufacturing processes. Martinez et al. [19] introduced an image-processing-based method capable of detecting flaws, irrespective of their orientation with respect to the surface textures from the machining operation. The decision-making is based on an algorithm that combines the extracted features under multiple lighting conditions. Frayman et al. [20] developed a hybrid genetic algorithm (GA)-based machine vision system for automated defect detection in die casting. An offline phase uses a GA to learn the image-processing parameters, based on which the online phase detects defects. Steiner and Katz [21] developed an image-processing algorithm to detect the porosity of machined components. This method does not require a template or training image set for defect detection. Other notable works have focused on techniques to identify chatter [22], grinding defects [23, 24], and circular defect patterns [25]. Although most of these techniques are capable of identifying surface features and defects, they are offline techniques used for fault detection and do not address how to improve the process.

The literature survey revealed that, although many studies have tried to address the issues of process stability and wire breakage in the WEDM process, none provided a process control technique based on wire wear. Because the relative degree of the wire wear is one of the indicators by which a potential wire

breakage can be detected, an algorithm to tune the process parameters based on wire wear can result in near-zero process interruptions. In addition, the existing image-processing techniques for feature detection have applications limited to the inspection of machined parts, and none has attempted a process control technique based on wire wear defined by imaging the wire surface. The objectives of the current study were as follows:

(a) To propose an image-processing algorithm for automatic detection and measurement of the wire wear rate

(b) To develop a WEDM process control system to tune the machining parameters, based on the extent of wire wear, to ensure continuous machining

3. Materials and Methods

3.1 Material selection

Inconel 718 was chosen as the work material because of its industrial significance in high-temperature applications. The material has high strength, fatigue, creep, and corrosion resistance, even at high temperatures [26]. The chemical and mechanical properties of Inconel 718 are listed in Tables 1 and 2, respectively. The wire electrode material selected was zinc-coated brass having a 0.25-mm diameter. Coated wires have been reported to have better overall performance than uncoated brass wires [27, 28].

Table 1 Chemical composition of Inconel 718 [26]

Element	**Ni**	**Fe**	**Cr**	**Nb**	**C**	**Al**	**Ti**	**Mo**
Weight (%)	Balancing	18.5	19	5.1	0.04	0.5	0.9	3

Table 2 Mechanical properties of Inconel 718 [29]

Property	**Value**
Density	8.19 g/cm^3
Melting point	1260 – 1336^{o}C
Specific heat	435 J/ (kg·K)
Coefficient of thermal expansion	13 μm / (m·K)
Thermal conductivity	11.4 W/(m·K)
Ultimate tensile strength	1240 MPa

3.2 Experimental setup and equipment

Electronica ECOCUT WEDM was used to machine the samples. The machine uses deionized water as the dielectric and has a resolution of 1 μm in every axis. A metallurgical microscope with 50-times

magnification was used to capture the wire wear data. A Zeiss Surfcom Flex 35-B surface profilometer was used to measure the average surface roughness of the machined specimen. A field-emission scanning electron microscope (Zeiss GeminiSEM 300) was used for the microstructural study. A schematic diagram of the experimental setup is presented in Fig. 1. Using this setup, the worn wire coming out from the machining zone is imaged using a microscope, and the captured raw image is sent to a computer for processing. The image-processing toolbox in MATLAB is used to preprocess and enhance the raw wire images. The processed image is used to quantify the degree of wire wear. Based on this, an algorithm recommends the parametric change to bring the process back to the ideal condition.

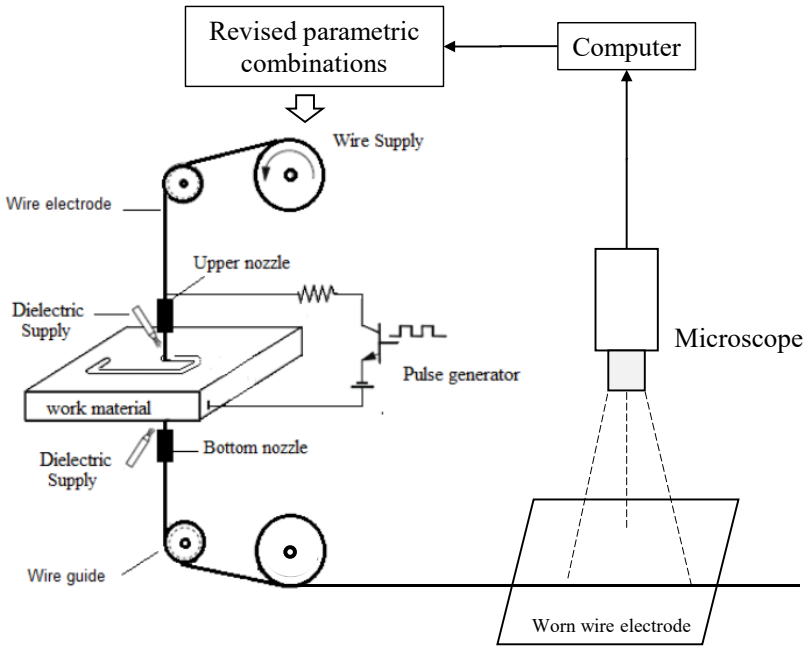

Fig. 1 Schematic of the experimental setup

3.3 Methodology

Experiments were conducted according to Taguchi's L_{18} orthogonal array with current, pulse on time, pulse off time, servo voltage, and wire feed rate as the input parameters. The current was varied in two levels and the rest of the parameters in three levels, as shown in Table 3. All other machining parameters were kept constant throughout the experimental investigation, as detailed in Table 4.

Table 3 Experimental settings of input parameters

Symbol	Parameters	Level 1	Level 2	Level 3
A	Input Current (A)	40	10	-
B	Pulse on time, T_{on} (μs)	100	105	110
C	Pulse off time, T_{off} (μs)	45	50	55
D	Servo voltage, SV (V)	45	50	55
E	Wire feed, WF (m/min)	3	5	7

Table 4. Constant machining parameters

Parameter	Value
Wire electrode type	Hard zinc coated brass
Wire electrode diameter	0.25 mm
Discharge voltage	12 V
Flushing pressure	1.96 bar
Wire Tension	10 N
Dielectric fluid	Deionized water

Digital image processing

Digital image processing is a technique in which a computer is used to perform a set of operations on a raw digital image to make it suitable for an application. For the current application, image processing is performed to quantify the wire wear. The various stages of the algorithm are illustrated in Fig. 2. First, the raw image is converted to a grayscale image. The operation excludes saturation and hue data and preserves the luminance data. The next operation is histogram equalization, which is a contrast enhancement tool used in image processing. This operator converts a grayscale image into an image with a specific number of gray levels. In this case, 1000 was selected as the number of gray levels. An equal number of pixels are distributed among the 1000 levels, making the histogram flatter than the original grayscale image. Fig. 3 shows the histogram comparison between the initial gray image and the equalized image in Fig. 2. The histogram equalized image is then converted to a binary image by setting a threshold value. The operator converts all pixel values above the threshold value to 1 and the others to 0. The threshold is specified as a scalar luminance value for this application. Finally, a disk-shaped morphological structuring element is used to erode and smoothen the image.

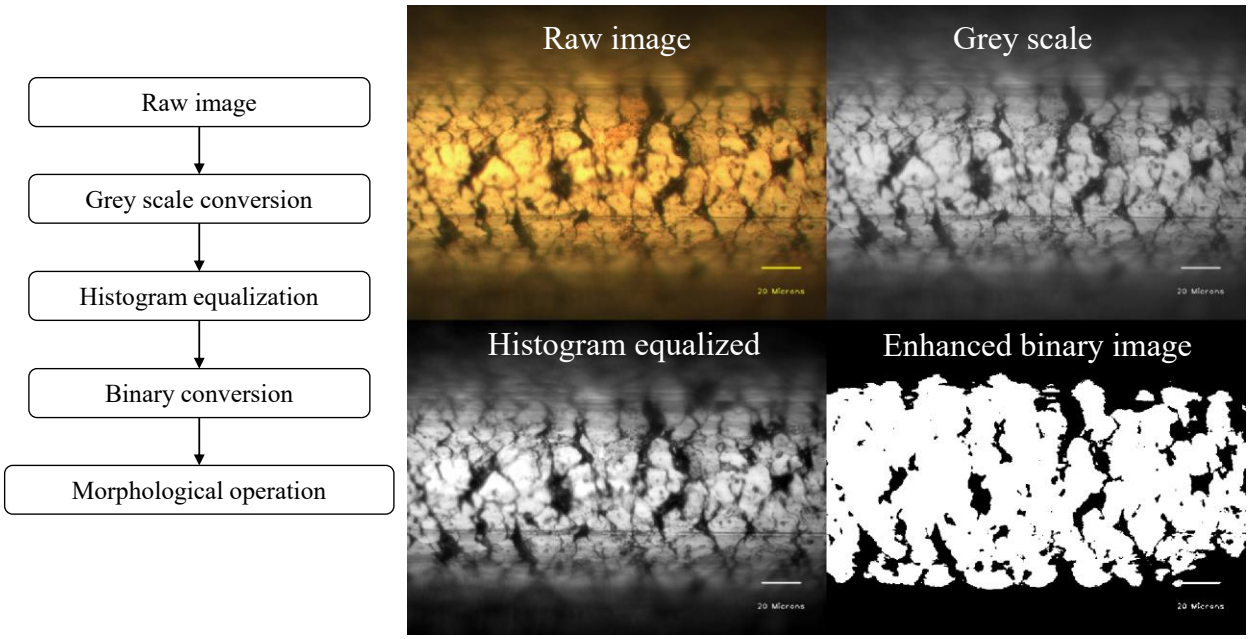

Fig. 2 Image processing operations

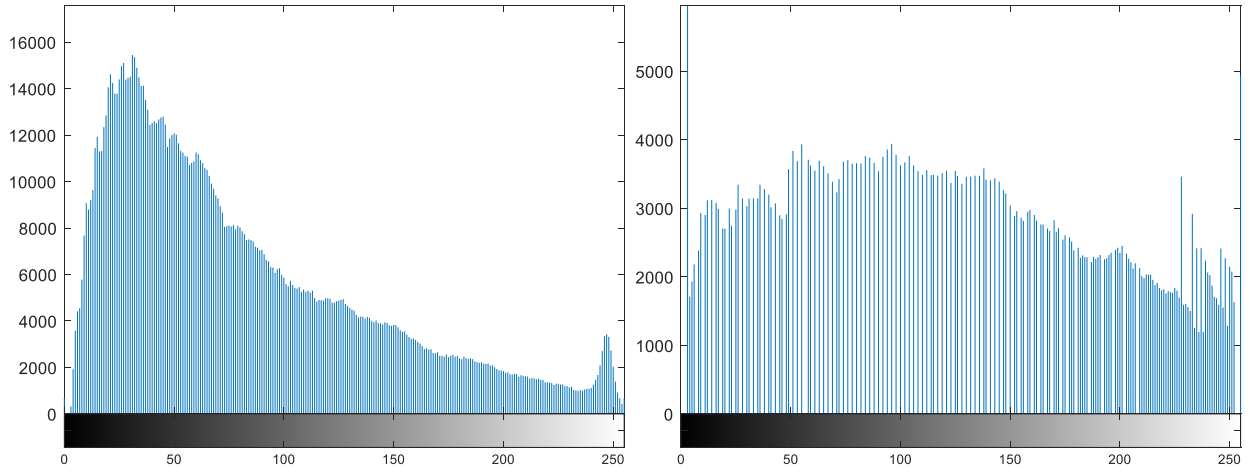

Fig. 3 Greyscale pixel histogram before and after equalization operation

To quantify the amount of wear in an electrode, it is sufficient to compare the worn wire with a fresh unused wire electrode. Thus, a fresh wire is processed to obtain an enhanced binary image, and the white pixel count is taken. The only visible surface features in a fresh wire electrode image are a few microcracks. A worn wire coming out of the machining zone definitely has fewer white pixels owing to the wire wear (which are seen as black pixels). A comparison of the enhanced binary images of the fresh and worn wires is shown in Fig. 4.

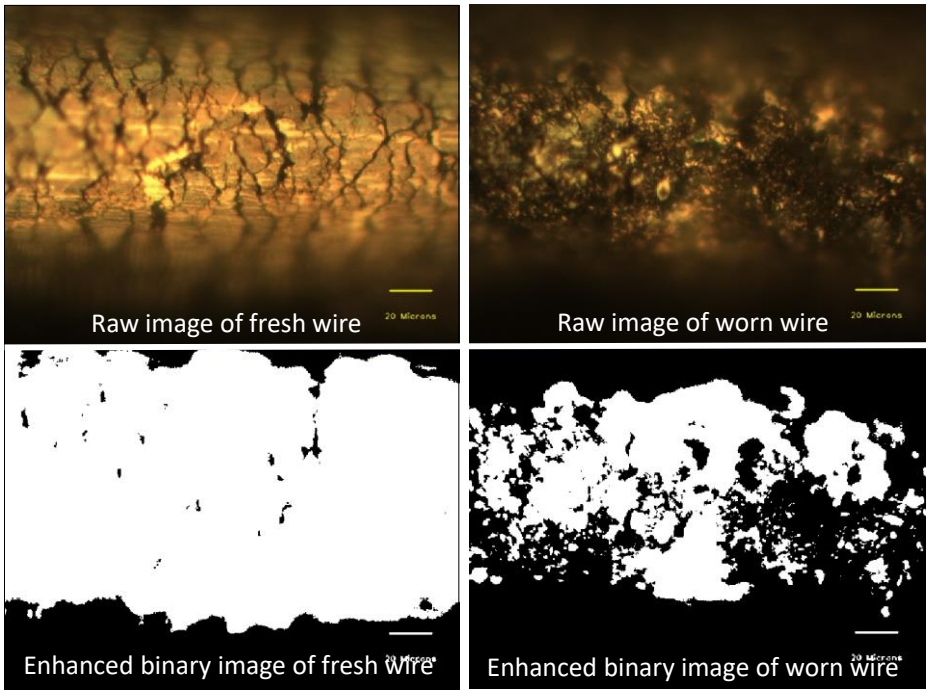

Fig. 4. Comparison of enhanced binary images of fresh and worn wire surfaces.

The wire wear ratio (WWR) is therefore calculated as follows:

$$WWR = \frac{(Total\ white\ pixel\ area\ in\ new\ wire - Total\ white\ pixel\ area\ in\ worn\ wire\ )}{(\ Total\ white\ pixel\ area\ in\ new\ wire\ )}$$

The WWR values for the two cases in Fig. 4 were calculated to be 0 and 0.537, respectively.

4. Results and Discussion

The experimental results of the L_{18} experimental runs are listed in Table 5. Three wire images were collected for each parameter setting, and the average WWR was calculated. In addition, the occurrence of wire breakages was recorded for each experimental run. Fig. 5 shows the graph of the wire wear rate against the experimental runs for all 18 cases. At higher wire wear rates, process interruptions through wire breakage were observed.

7

Table 5 Experimental design and corresponding responses

S. No	Input parameters					1	Responses				
							Wire wear ratio (WWR)			WWR	Wire breakage
	Current (A)	T_{ON} (µs)	T_{OFF} (µs)	SV (V)	WF (mm/min)		Trial 1	Trial 2	Trial 3		
1	40	100	45	45	3		0.16	0.214	0.231	0.202	×
2	40	100	50	50	5		0.03	0.035	0.038	0.034	×
3	40	100	55	55	7		0.011	0.007	0.014	0.011	×
4	40	105	45	45	5		0.574	0.534	0.502	0.537	✓
5	40	105	50	50	7		0.471	0.454	0.557	0.494	✓
6	40	105	55	55	3		0.459	0.357	0.432	0.416	✓
7	40	110	45	50	3		0.425	0.455	0.613	0.498	✓
8	40	110	50	55	5		0.435	0.436	0.391	0.421	✓
9	40	110	55	45	7		0.502	0.573	0.432	0.502	✓
10	10	100	45	55	7		0.057	0.184	0.085	0.109	×
11	10	100	50	45	3		0.13	0.202	0.151	0.161	×
12	10	100	55	50	5		0.021	0.035	0.028	0.028	×
13	10	105	45	50	7		0.251	0.266	0.203	0.240	×
14	10	105	50	55	3		0.074	0.079	0.083	0.079	×
15	10	105	55	45	5		0.147	0.178	0.121	0.149	×
16	10	110	45	55	5		0.057	0.085	0.061	0.068	×
17	10	110	50	45	7		0.164	0.128	0.233	0.175	×
18	10	110	55	50	3		0.336	0.399	0.32	0.352	✓

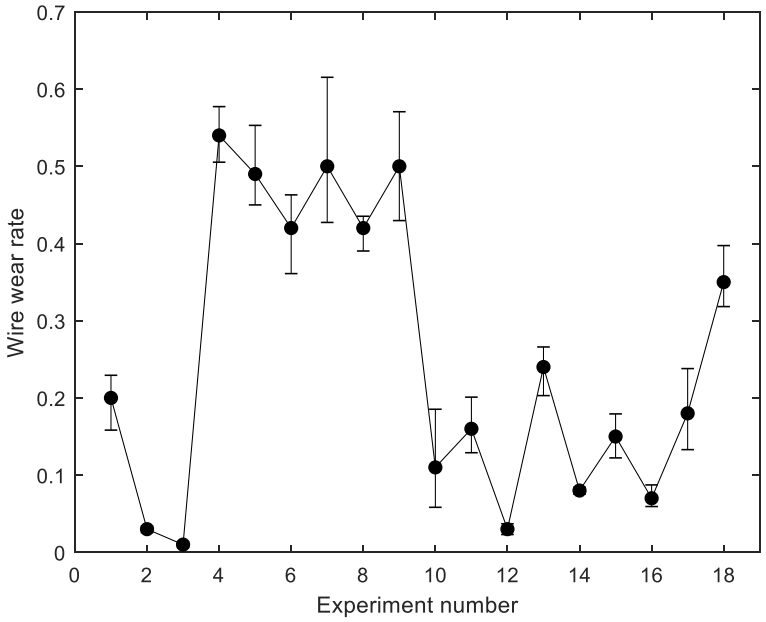

Fig. 5. Wire wear ratio for different parameter combinations

4.1 Effect of process parameters on wire wear

The material removal mechanism of the WEDM process involves spark erosion, resulting in the melting and vaporization of the electrodes. Material removal occurs from the wire and workpiece electrodes, even though the material from the workpiece is relatively high. The constant wearing off of the wire surface is the reason why the fresh wire is continuously fed to the machining zone from a wire spool. The primary factors that affect the WWR are the discharge current, pulse on time, pulse off time, servo voltage, and wire feed rate. Fig. 6 and Table 6 show the main effects plot and response table for the WWR, respectively. The response table shows that the WWR is maximally affected by the pulse on time, followed by the discharge current and servo voltage.

The WWR increases as the discharge current and pulse on time increase. These parameters are directly proportional to the discharge energy of the spark, given by

$$D_e = I_e.V_e.T_e$$

where D_e is the discharge energy of the spark, I_e is the discharge current, V_e is the voltage, and T_e is the discharge duration. The discharge duration increased as the pulse on time increased. Thus, the discharge energy increases with the pulse on time and discharge current. At higher discharge energies, the instantaneous temperature on the wire electrode was greater, resulting in more wire wear by melting and vaporization.

Fig. 6 Main effects plot for wire wear ratio

9

Table 6 Response table for wire wear ratio

Level	I_P	T_{on}	T_{off}	SV	WF
1	0.34611	0.09083	0.27567	0.28767	0.28467
2	0.15122	0.31917	0.22733	0.27433	0.20617
3		0.33600	0.24300	0.18400	0.25517
Delta	0.19489	0.24517	0.04833	0.10367	0.07850
Rank	2	1	5	3	4

The interelectrode gap between the wire and the workpiece is controlled by the servo voltage. The higher the servo voltage, the greater is the spark gap. The discharge energy of the spark is distributed to the workpiece, dielectric, and wire electrode. The energy that enters the workpiece contributes to material removal. As the spark gap increases, the discharge energy lost into the dielectric increases; thus, the part of the discharge energy that goes to both electrodes is reduced. This is the reason why the WWR is lower at higher servo voltage values. The pulse off time and wire feed rate do not show any particular trend in how they affect the WWR. However, generally, a shorter pulse off time is detrimental to machining stability because it causes gap bridging and short-circuit pulses. These arc and short-circuit pulses are associated with higher-than-ideal localized temperature zones, resulting in higher wire wear and excessive thermal softening. The reduced wire strength caused by the thermal impact results in eventual wire breakage. In addition, a very low wire feed rate can increase the WWR because the chances of repeated sparks from a single wire location are higher.

4.2 Process control algorithm

Wire breakages are directly related to the spark gap instabilities. The mechanism of wire breakage involves excessive thermal load on the wire, which can be identified by high relative wire wear resulting in cracks/craters. In the case of coated wires, the thermal load is greater when the coating is removed because the "heat sink effect" is not present to protect the inner core from thermal damage. Thus, the wire loses its strength to withstand the wire tension, causing wire breakage. Therefore, to maintain process continuity and stability, it is sufficient to monitor the wire wear. Based on this concept, a process control algorithm was developed, as shown in Fig. 7. Most cases of machining failures are associated with debris accumulation in the spark gap, leading to spark gap bridging. Three factors contribute to the gap bridging: insufficient time to clear the debris from the spark gap (less T_{off}), an insufficient gap between the electrode for proper flushing (less SV), and wire travel that is too slow to stagnate the spark gap (less WF). The algorithm can adjust the aforementioned process parameters based on the degree of wire wear.

The algorithm aims to suppress the debris accumulation tendency at an optimal level so that the responses are least affected. The algorithm works to enhance the spark gap condition in three ways.

- It incrementally increases the time available to flush away the debris from the Inter electrode gap ~~IEG~~ (i.e., by increasing the pulse off time, T_{OFF}).
- It incrementally increases the spark gap distance to facilitate debris clearance (i.e., by increasing the servo voltage, SV).
- It incrementally increases the wire feed rate to reduce the concentrated thermal load.

The conditions are applied based on the severity of instability. For instance, when there is less wire wear, only the first condition is applied. Every incremental step is fixed such that the responses are affected minimally, and process control is performed only at the point where wire breakage is avoided. By applying the algorithm for process control, the overall productivity is enhanced because the time lost for wire rethreading is much greater in the case of wire breakage. In addition, wire breaks can lead to machined part rejection resulting from surface damage and geometric inaccuracies.

Based on the severity of wire wear, the algorithm revises the process parameters as follows.

- Low-severity wire wear ($0.3 < WWR < 0.4$): The pulse off time is increased by 5 µs. This provides more time to clear the debris and reduces the spark gap bridging.

- Medium-severity wire wear ($0.4 < WWR < 0.5$): The pulse off time is increased by 5 µs, and the servo voltage is increased by 5 V. Not only the time of flushing, but also the interelectrode gap is increased, enabling the debris to be cleared from the machining zone.

- High-severity wire wear ($WWR > 0.5$): The pulse off time is increased by 5 µs, the servo voltage is increased by 5 V, and the wire feed rate is increased by 3 m/min. In addition to the increase in the spark gap and flushing time, the wire feed rate is increased. An increase in the wire feed rate has multiple effects. First, it helps provide flushability. Second, it prevents localized thermal load and wire wear, which can lead to failure. If the wire moves through the machining zone faster, there are fewer chances of repetitive sparks from the same spot.

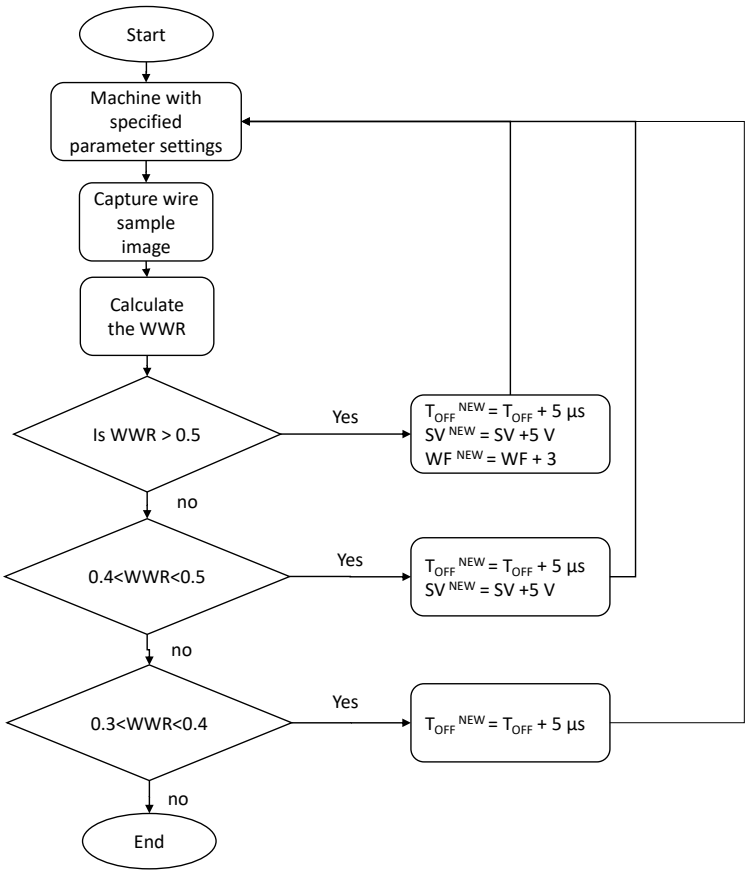

Fig. 7 Algorithm for process control based on degree of wire wear

11

Table 7 shows the effect of process control on the machining outcome and performance characteristics. In the wire breakage cases considered, every experimental run resulted in a machining failure within 10.31 mm. The earliest occurrence of wire breakage was reported after a machining length of 1.32 mm (Exp. No. 9). To study the improvement in process control, a total machining length of 100 mm was considered. The controlled settings ensured continuous machining for the entire 100-mm length. The process control not only avoided wire breakages but also improved the surface finish of the machined parts. This is because of the improved flushing conditions after process control, resulting in the reduction of harmful sparks (short circuits and arcs). Owing to process control, an average reduction of 10.82 % was obtained for the surface roughness.

The machining speed after process control was slightly lower than the original speed because the pulse off time increased during process control. However, compared with the time taken for wire rethreading after wire breakage, the reduction in cutting speed was marginal and can be justified. An average cutting speed reduction of 8.2% occurred owing to process control.

Table 7 Parameter adjustments based on process control algorithm to avoid wire breakages

ITERATION 1

S. No	WWR	WB	CS (mm/min)	Ra (µm)	ML (mm)
4	0.537	Yes	2.38	3.66	2.37
5	0.494	Yes	2.01	3.05	5.31
6	0.416	Yes	1.87	2.75	7.89
7	0.498	Yes	2.11	3.16	4.11
8	0.421	Yes	1.74	1.95	8.74
9	0.502	Yes	1.98	3.57	1.32
18	0.352	Yes	1.63	2.53	10.31

ITERATION 2

S. No	WWR	WB	CS (mm/min)		Ra (µm)		ML (mm)	
			Original	After PC	Original	After PC	Original	After PC
4	0.129	No	2.38	2.15	3.66	3.12	2.31	100
5	0.412	Yes	2.01	1.86	3.05	2.91	5.31	21.2
6	0.274	No	1.87	1.75	2.75	2.41	7.89	100
7	0.421	Yes	2.11	1.97	3.16	2.81	4.11	18.7
8	0.182	No	1.74	1.59	1.95	1.84	8.74	100
9	0.208	No	1.98	1.74	3.57	3.21	1.32	100
18	0.156	No	1.63	1.42	2.53	2.2	10.31	100

ITERATION 3

S. No	WWR	WB	CS (mm/min)		Ra (µm)		ML (mm)	
			Original	After PC	Original	After PC	Original	After PC
5	0.122	No	2.01	1.93	2.91	2.51	21.2	100
7	0.161	No	2.11	1.98	2.81	2.47	18.7	100

WWR – Wire Wear Ratio, WB – Wire Breakage, CS – Cutting Speed, Ra – Average surface roughness, PC – Process control, ML – Machined length

12

4.3 Discharge pulse analysis

In the electrical discharge machining process, the discharge pulses are classified into spark, arc, short-circuit, and open-circuit pulses. After the voltage is applied across the electrodes, a pulse is called a “spark pulse” if a current pulse occurs after an ignition delay time. If the ignition delay time is too low or absent and the current pulse occurs as soon as the voltage pulse reaches the peak, the pulse is an arc pulse. If the current pulse occurs without any voltage peaks, such sparks are called “short-circuit sparks.” If the voltage is applied for a longer duration without the current spark, it is called an “open-circuit spark.” The different pulse types are shown in Fig. 8.

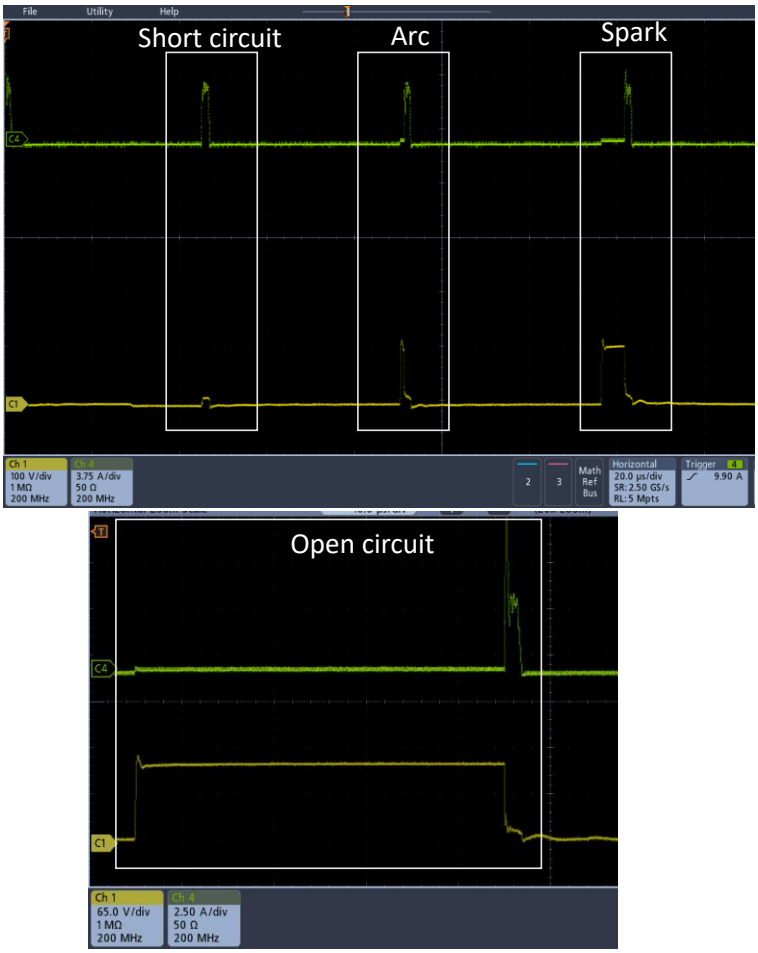

Fig. 8 Different types of pulse discharges

Ideally, all discharges in the WEDM pulse cycle are spark discharges. However, every pulse cycle consists of all four pulse types in varying proportions. The presence of an arc pulse increases the material removal rate but creates a rougher surface. Open-circuit discharges decrease productivity and make machining inefficient. Short-circuit discharges are considered undesirable or abnormal and are reported to be the main reason for wire breakage. Short circuits are caused by debris accumulation and spark gap

bridging, producing higher-intensity sparks. This results in significant wire damage, eventually leading to breakage [30].

The discharge pulse proportions were analyzed for various wire wear situations, as shown in Fig. 9. They were computed by a pulse classifier based on the ignition delay time. Under normal machining conditions without any breakages, the spark discharge pulses dominated the pulse cycle. For the maximum wire wear rate condition (WWR > 0.5), the proportion of short-circuit pulses is higher. Moreover, the proposed process control algorithm resulted in a pulse cycle with a higher proportion of spark discharges through parameter modifications. This ensures failure-free continuous machining, as shown in Table 7.

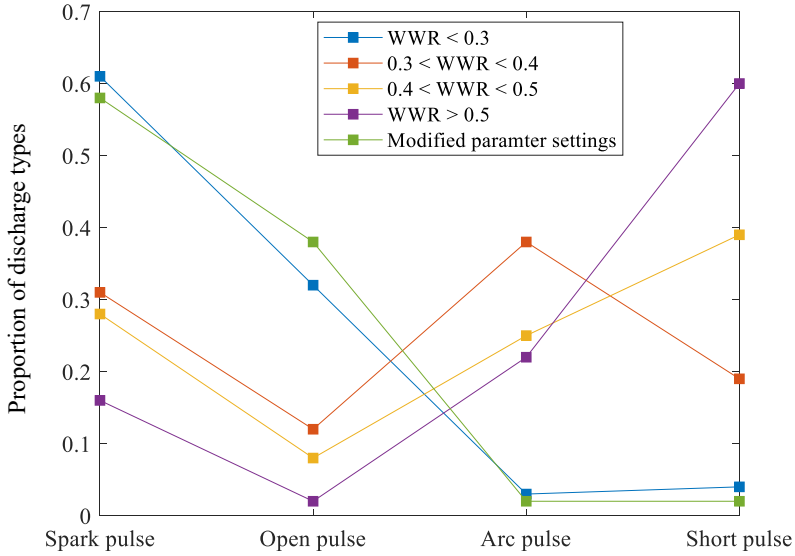

Fig. 9 Discharge pulse proportions for various wire wear ratios

4.4 Microstructural analysis

Scanning electron microscopy (SEM) images of the worn wire surfaces were compared to verify the effect of the process control algorithm, as shown in Fig. 10. Fig. 10(a) shows the case of Exp. No. 4 with a 0.537 WWR. The wire surface severely deteriorated, with the zinc coating removed in many places. However, after process control was applied, the revised settings caused minimal wire wear, as shown in Fig. 10(b). The wire coating was still intact, with only minor damage. This was validated by performing energy dispersive X-ray analysis (EDS) of the wire samples. Fig. 11(a) shows that, corresponding to Exp. No. 4, the zinc proportion was 65.06%, compared with 87.41% after process control (Fig. 11(b)). The higher percentage of zinc was caused by the restoration of machining stability, resulting in reduced wire wear in comparison with the original process settings. This confirms the ability of the control algorithm to restore process stability and avoid wire break failures.

14

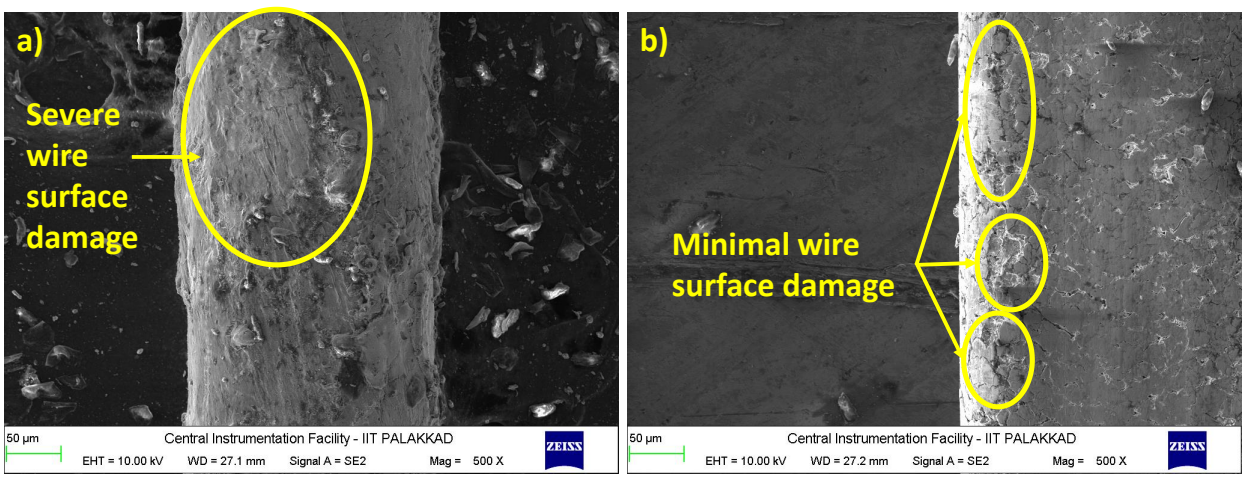

Fig. 10 SEM images of worn wore surfaces at (a) Original process conditions leading to failure (Exp. No. 4) (b) Revised machining conditions according to control algorithm

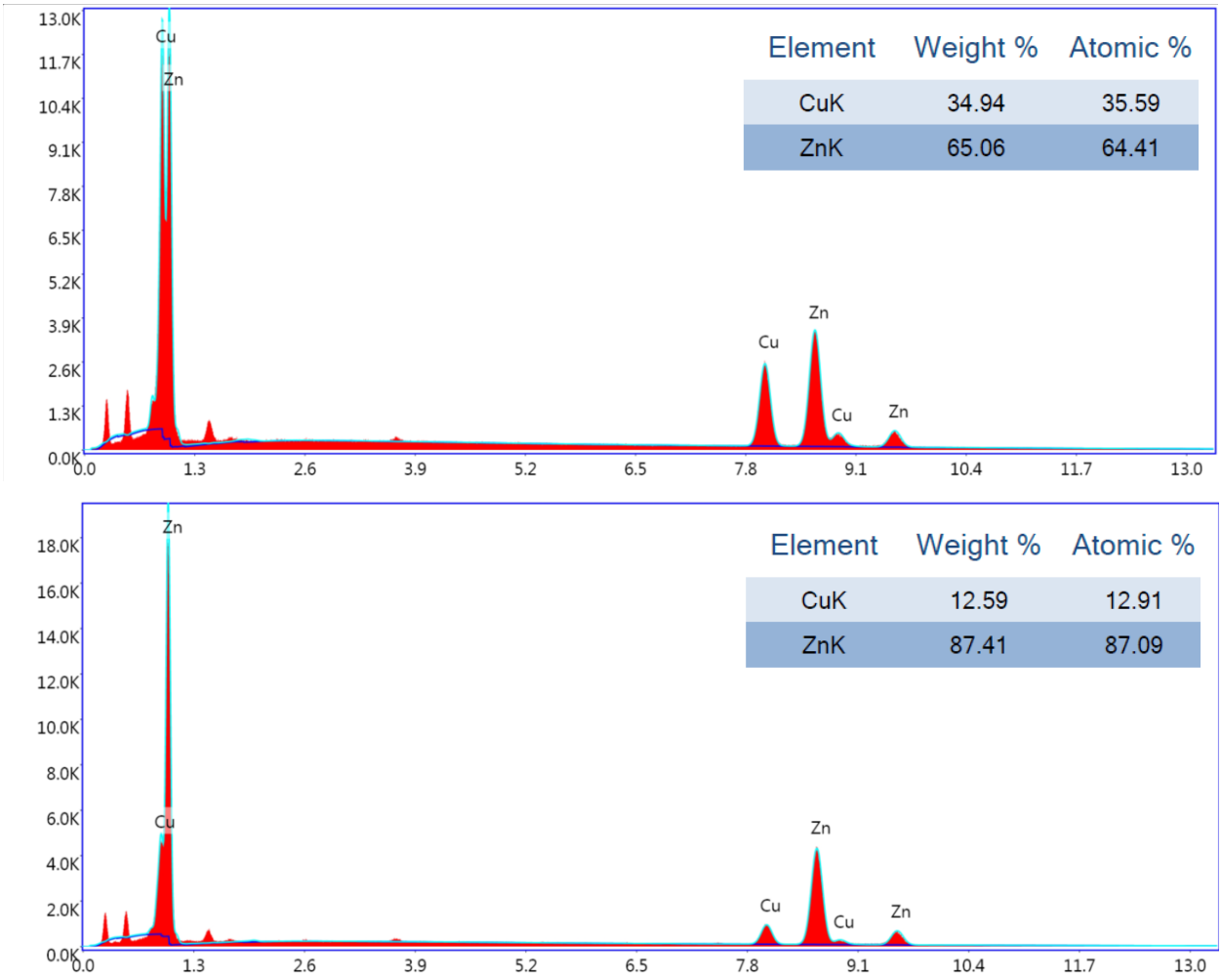

Fig. 11 EDS analysis of worn wore surfaces at (a) Original process conditions leading to failure (Exp. No. 4) (b) Revised machining conditions according to control algorithm

15

5. Conclusions

The WEDM process has several merits over traditional machining, especially during the machining of superalloys. However, process efficiency is still a concern owing to frequent wire breakages. Failure prediction and control algorithms are extremely relevant from an industrial point of view to reduce machine downtime and increase productivity. A machine-vision-based wire wear analysis system for WEDM process control was presented in this report.

A method for quantifying wire wear was developed using an image-processing technique. The microscopic image of the wire surface is preprocessed, enhanced, and analyzed to compute a response variable, the WWR. The causes of the increased WWR were investigated, and parametric dependency studies were conducted. The pulse on time and discharge current were found to have the greatest effect on wire wear. A process control algorithm was developed that fine tunes the process parameters to reduce wire wear. The cases of wire breakage can be identified in advance, and failure can be avoided using this methodology. The effectiveness of the algorithm was further verified by analyzing the discharge pulse proportions and through microstructural analysis.

Declarations

Funding The authors declare that no funding was received for this study.

Conflicts of interest/Competing interests The authors declare that they have no known competing financial interests or personal relationships that have influenced the current work.

Availability of data and material All the data are available in the article.

Code availability Not applicable

Acknowledgment

The authors would like to thank the central instrumentation facility (CIF), IIT Palakkad, for providing the test facility and equipment.

References

1. Ho KH, Newman ST, Rahimifard S, Allen RD (2004) State of the art in wire electrical discharge machining (WEDM). Int J Mach Tools Manuf 44:1247–1259. https://doi.org/10.1016/j.ijmachtools.2004.04.017

2. Mandal A, Dixit AR (2014) State of art in wire electrical discharge machining process and performance. Int J Mach Manu Mater 16:1. https://doi.org/10.1504/IJMMM.2014.063918

3. Ramakrishnan R, Karunamoorthy L (2008) Modeling and multi-response optimization of Inconel 718 on machining of CNC WEDM process. J Mater Process Technol 207:343–349. https://doi.org/10.1016/j.jmatprotec.2008.06.040

4. Mandal A, Dixit AR, Das AK, Mandal N (2016) Modeling and Optimization of Machining Nimonic C-263 Superalloy using Multicut Strategy in WEDM. Mater Manuf Process 31:860–868. https://doi.org/10.1080/10426914.2015.1048462

5. Manjaiah M, Laubscher RF, Kumar A, Basavarajappa S (2016) Parametric optimization of MRR and surface roughness in wire electro discharge machining (WEDM) of D2 steel using Taguchi-based utility approach. Int J Mech Mater Eng 11: https://doi.org/10.1186/s40712-016-0060-4

6. Senkathir S, Aravind R, Samson RM, Raj ACA (2019) Optimization of Machining Parameters of Inconel 718 by WEDM Using Response Surface Methodology. Adv Manuf Process 383–392. https://doi.org/10.1007/978-981-13-1724-8

7. Bergs T, Tombul U, Herrig T, et al (2018) Analysis of Characteristic Process Parameters to Identify Unstable Process Conditions during Wire EDM. Procedia Manuf 18:138–145. https://doi.org/10.1016/j.promfg.2018.11.018

8. Gamage JR, Desilva AKM (2016) Effect of Wire Breakage on the Process Energy Utilisation of EDM. Procedia CIRP 42:586–590. https://doi.org/10.1016/j.procir.2016.02.264

9. Kawata A, Okada A, Okamoto Y, Kurihara H (2017) Influence of nozzle jet flushing on wire breakage in 1st-cut wire edm from start hole. Key Eng Mater 749 KEM:130–135. https://doi.org/10.4028/www.scientific.net/KEM.749.130

10. Melnik Y, Kozochkin M, Porvatov A, Okunkova A (2018) On Adaptive Control for Electrical Discharge Machining Using Vibroacoustic Emission. Technologies 6:96. https://doi.org/10.3390/technologies6040096

11. Kwon S, Yang MY (2006) The benefits of using instantaneous energy to monitor the transient state of the wire EDM process. Int J Adv Manuf Technol 27:930–938. https://doi.org/10.1007/s00170-004-2252-y

12. Yan MT, Liao YS (1996) A self-learning Fuzzy controller for wire rupture prevention in WEDM. Int J Adv Manuf Technol 11:267–275. https://doi.org/10.1007/BF01351284

13. Yan MT, Liao YS (1998) Adaptive Control of the WEDM Process Using the Fuzzy Control Strategy. J Manuf Syst 17:263–274

14. Liao YS, Woo JC (2000) Design of a fuzzy controller for the adaptive control of WEDM process. Int J Mach Tools Manuf 40:2293–2307. https://doi.org/10.1016/S0890-6955(00)00036-5

15. Bufardi, Ahmed and Akten, Olcay and Arif, Muhammad and Xirouchakis, Paul and Perez, Roberto (2017) Towards zero-defect manufacturing with a combined online - offline fuzzy-nets approach in wire electrical discharge machining. WSEAS Transactions on Environment and Development, 13. pp. 401-409. ISSN 1790-5079

16. Caggiano A, Teti R, Perez R, Xirouchakis P (2015) Wire EDM monitoring for zero-defect manufacturing based on advanced sensor signal processing. Procedia CIRP 33:315–320. https://doi.org/10.1016/j.procir.2015.06.065

17. Cabanes I, Portillo E, Marcos M, Sánchez JA (2008) On-line prevention of wire breakage in wire electro-discharge machining. Robot Comput Integr Manuf 24:287–298. https://doi.org/10.1016/j.rcim.2006.12.002

18. Klocke F, Welling D, Klink A, Perez R (2014) Quality assessment through in-process monitoring of wire-EDM for fir tree slot production. New Prod Technol Aerosp Ind - 5th Mach Innov Conf (MIC 2014)-Procedia CIRP 24:97–102. https://doi.org/10.1016/j.procir.2014.07.136

19. Martínez SS, Vázquez CO, García JG, Ortega JG (2015) Image fusion for surface finishing inspection. IST 2015 - 2015 IEEE Int Conf Imaging Syst Tech Proc 3–8. https://doi.org/10.1109/IST.2015.7294579

20. Frayman Y, Zheng H, Nahavandi S (2006) Machine Vision System for Automatic Inspection of Surface Defects in Aluminum Die Casting. J Adv Comput Intell Intell Informatics 10:281–286. https://doi.org/10.20965/jaciii.2006.p0281

21. Steiner D, Katz R (2007) Measurement techniques for the inspection of porosity flaws on machined surfaces. J Comput Inf Sci Eng 7:85–94. https://doi.org/10.1115/1.2424244

22. Khalifa OO, Densibali A, Faris W (2006) Image processing for chatter identification in machining processes. Int J Adv Manuf Technol 31:443–449. https://doi.org/10.1007/s00170-005-0233-4

23. Manish R, Venkatesh A, Denis Ashok S (2018) Machine Vision Based Image Processing Techniques for Surface Finish and Defect Inspection in a Grinding Process. Mater Today Proc 5:12792–12802. https://doi.org/10.1016/j.matpr.2018.02.263

24. Zhang C, Zhang J (2013) On-line tool wear measurement for ball-end milling cutter based on machine vision. Comput Ind 64:708–719. https://doi.org/10.1016/j.compind.2013.03.010

25. Tsai DM, Rivera Molina DE (2019) Morphology-based defect detection in machined surfaces with circular tool-mark patterns. Meas J Int Meas Confed 134:209–217. https://doi.org/10.1016/j.measurement.2018.10.079

26. Reed RC (2006) The Superalloys Fundamentals and Applications. Cambridge University Press

27. Ramamurthy A, Sivaramakrishnan R, Muthuramalingam T, Venugopal S (2015) Performance Analysis of Wire Electrodes on Machining Ti-6Al-4V Alloy using Electrical Discharge Machining Process. Mach Sci Technol 19:577–592. https://doi.org/10.1080/10910344.2015.1085314

28. Maher I, Sarhan AAD, Hamdi M (2014) Review of improvements in wire electrode properties for longer working time and utilization in wire EDM machining. Int J Adv Manuf Technol 76:329–351. https://doi.org/10.1007/s00170-014-6243-3

29. Thakur DG, Ramamoorthy B, Vijayaraghavan L (2009) Study on the machinability characteristics of superalloy Inconel 718 during high speed turning. Mater Des 30:1718–1725. https://doi.org/10.1016/j.matdes.2008.07.011

30. Abhilash PM, Chakradhar D (2020) Surface integrity comparison of wire electric discharge machined Inconel 718 surfaces at different machining stabilities. Procedia CIRP 87:228–233. https://doi.org/10.1016/j.procir.2020.02.037

AUTHOR CV

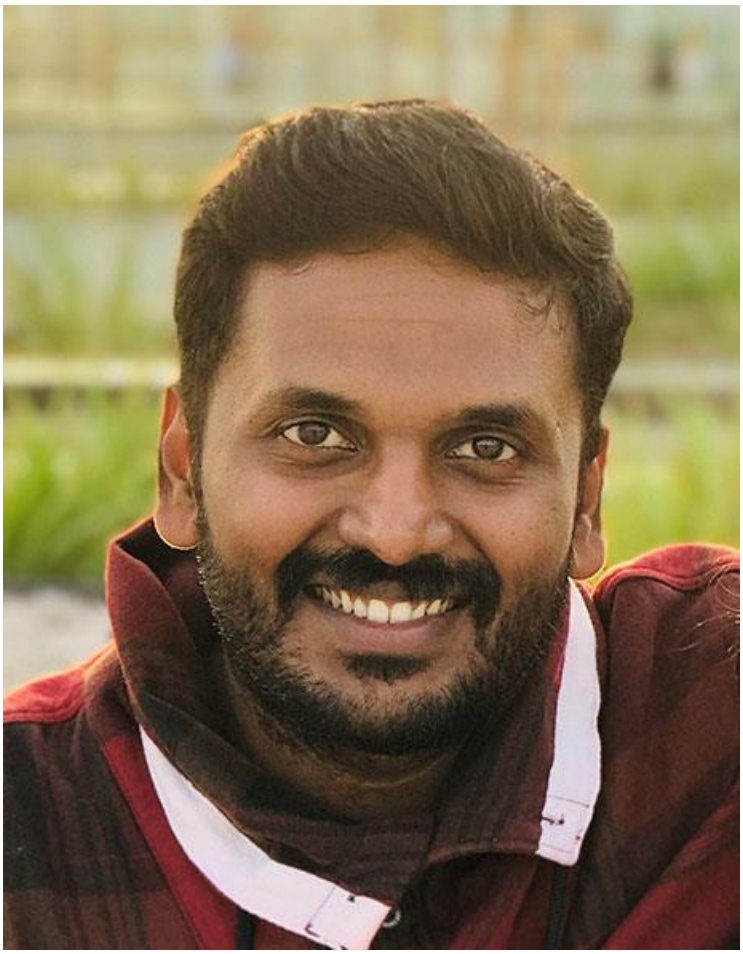

Mr. Abhilash P. M. is currently pursuing doctoral degree in the Discipline of Mechanical Engineering at Indian institute of Technology Palakkad, India. He has completed Master's degree in Engineering Design from Amrita Vishwa Vidyapeetham, Coimbatore, India. His areas of interests are smart manufacturing, process condition monitoring, signal processing, image processing, advanced process optimization and application of artificial intelligence in manufacturing. He has currently published seven international journals.

Dr. D. Chakradhar is currently working as an Assistant Professor in the Discipline of Mechanical Engineering at Indian institute of Technology Palakkad, India. He has completed M. Tech. in Advanced Manufacturing Processes and Ph.D. in Mechanical Engineering from National Institute of Technology Warangal, India. His areas of interest are non-traditional machining, cryogenic machining and artificial intelligence in manufacturing. He has contributed to more than forty publications in international journals/conference proceedings.